NeuroImage 172 (2018) 654–662

Contents lists available at ScienceDirect

NeuroImage

journal homepage: www.elsevier.com/locate/neuroimage

Temporal recalibration of motor and visual potentials in lag adaptation in voluntary movement

Chang Cai [a,b,*], Kenji Ogawa [a,c], Takanori Kochiyama [d], Hirokazu Tanaka [e], Hiroshi Imamizu [a,b,f,**]

[a] Cognitive Mechanisms Laboratories, Advanced Telecommunications Research Institute International, Keihanna Science City, Kyoto 619-0288, Japan
[b] Center for Information and Neural Networks, National Institute of Information and Communications Technology and Osaka University, Suita, Osaka 565-0871, Japan
[c] Department of Psychology, Graduate School of Letters, Hokkaido University, Sapporo, Hokkaido 060-0810, Japan
[d] Brain Activity Imaging Center, ATR-Promotions, Keihanna Science City, Kyoto 619-0288, Japan
[e] School of Information Science, Japan Advanced Institute of Science and Technology, Nomi, Ishikawa 923-1211, Japan
[f] Department of Psychology, Graduate School of Humanities and Sociology, The University of Tokyo, Tokyo 113-0033, Japan

ARTICLE INFO

Keywords:
Lag adaptation
Readiness potential
Visually evoked potential
Voluntary movement

ABSTRACT

Adaptively recalibrating motor-sensory asynchrony is critical for animals to perceive self-produced action consequences. It is controversial whether motor- or sensory-related neural circuits recalibrate this asynchrony. By combining magnetoencephalography (MEG) and functional MRI (fMRI), we investigate the temporal changes in brain activities caused by repeated exposure to a 150-ms delay inserted between a button-press action and a subsequent flash. We found that readiness potentials significantly shift later in the motor system, especially in parietal regions (average: 219.9 ms), while visually evoked potentials significantly shift earlier in occipital regions (average: 49.7 ms) in the delay condition compared to the no-delay condition. Moreover, the shift in readiness potentials, but not in visually evoked potentials, was significantly correlated with the psychophysical measure of motor-sensory adaptation. These results suggest that although both motor and sensory processes contribute to the recalibration, the motor process plays the major role, given the magnitudes of shift and the correlation with the psychophysical measure.

Introduction

To achieve an intentional goal, we usually need to perform a series of adaptive actions in voluntary movement. Every action has a subsequent outcome, and adaptively and precisely synchronizing the outcome with the action is essential for all living animals. For example, a moving animal must distinguish the sound of its walking from environmental sounds in order to remain alert to nearby predators (Stetson et al., 2006). This synchrony may be confounded by changes of delay in motor circuits (e.g., fatigue) or sensory circuits (e.g., slow response of mouse cursor due to computer overload), and the brain must continuously recalibrate such asynchrony. Adaptation to a motor-sensory lag, in which the perceived time between an action and a delayed consequence is compressed after repeated exposures to the delay, is an example of such recalibration (Haggard, 2005; Stetson et al., 2006).

In voluntary movement, it is controversial whether the recalibration resulting from sensory lag adaptation occurs in sensory or motor circuits. One theory hypothesizes that the perceived timing of a sensory event shifts earlier to the timing of an action in delay condition than in no-delay condition (Cai et al., 2012; Stetson et al., 2006). This theory is based on an illusory reversal of action and outcome: Participants perceive that sensory events occur before their actions when the delay is unexpectedly removed after the adaptation. This suggests the importance of calibration in sensory circuits after sensory events (retrospective processes).

Another theory suggests the importance of prospective processes within motor-related circuits (Haggard, 2014). This is supported by findings that outcome predictability (Haggard et al., 2002; Moore and Haggard, 2008) prior to the action is necessary for the 'intentional binding' effect (Haggard et al., 2002), which refers to the subjective compression of an interval between a voluntary action and a delayed

* Corresponding author. Cognitive Mechanisms Laboratories, Advanced Telecommunications Research Institute International, Keihanna Science City, Kyoto 619-0288, Japan.
** Corresponding author. Department of Psychology, Graduate School of Humanities and Sociology, The University of Tokyo, Tokyo 113-0033, Japan.
E-mail addresses: cai.fmri@gmail.com (C. Cai), imamizu@l.u-tokyo.ac.jp (H. Imamizu).

https://doi.org/10.1016/j.neuroimage.2018.02.015
Received 27 May 2017; Received in revised form 11 December 2017; Accepted 7 February 2018
Available online 8 February 2018

outcome. Another psychophysical study reported a transfer of adaptation effect between motor-visual and motor-auditory asynchrony, suggesting the motor system's involvement in lag adaptation (Sugano et al., 2010).

However, to our knowledge, it is unknown which components in a motor-related process change according to the recalibration. Previous studies have suggested that our awareness of movement is derived from signals that precede the movements rather than sensory feedback from a moving limb (Blakemore and Frith, 2003; Libet et al., 1983). Readiness potentials are well-known neural signals that precede movements (Kornhuber and Deecke, 1965; Shibasaki and Hallett, 2006). Moreover, previous studies suggested the importance of Brodmann area (BA) 6 (including premotor and supplementary motor areas) and parietal regions to motor intention (Haggard, 2008; Lau et al., 2004) and preparation (Wheaton et al., 2005). Therefore, we hypothesized that a significant change due to recalibration could be found in the readiness potentials in BA 6 and parietal regions in cases where a prospective process contributes to the recalibration.

To examine this hypothesis, we investigated how readiness potentials, which gradually increase toward the onset of voluntary movement (a button press in this study), change in BA 6 and parietal regions due to lag adaptation. We used MEG for measurement of the magnetic signals related to the readiness potentials and estimated the source cortical currents from the MEG signals in combination with fMRI measurements. We also investigated changes in the retrospective sensory-related circuits. Specifically, we investigated visually evoked potentials whose main sources have been localized in the occipital lobe (BA 17/18/19) (Di Russo et al., 2002). Although previous studies (Di Luca et al., 2009; Keetels and Vroomen, 2008) found changes in tactile and proprioceptive perception in lag adaptation, we mainly investigated changes in visually evoked potentials that are directly related to the delayed sensory consequence (a flash in this study). We found that, although both the prospective motor process and the retrospective sensory process contribute to the recalibration, the motor process preceding the movements in parietal regions seems to play the major role, considering the magnitudes of the shift and the correlation with the psychophysical measure of the adaptation.

Materials and methods

Experimental design

We measured brain activities using MEG while participants voluntarily pressed a button and observed a consequent flash in delay and no-delay conditions (see Supplementary Fig. 1 for a graphical overview of our experimental design). fMRI activity in a voluntary button-press task was measured to estimate cortical source currents from the MEG signals. From the estimated cortical currents, we identified readiness currents (corresponding to readiness potentials in electroencephalogram measurement) and estimated temporal shifts of the currents due to a lag adaptation. Temporal shifts of flash-evoked currents (visually evoked currents, corresponding to visually evoked potentials in electroencephalogram measurement) were also estimated within the visual cortex. Next, we tested the statistical significance of shifts in readiness and evoked currents, as well as the correlation between the degree of current shifts and a psychophysical measure of lag adaptation obtained from a temporal order judgment task following the voluntary button-press task.

Participants

Sixteen right-handed male participants (aged 20–45 years, mean 25.1) participated in this study. A signed informed consent form was obtained from each participant. The experiments were conducted according to the Declaration of Helsinki and approved by the Ethics Committee at Advanced Telecommunication Research Institute International (http://www.atr.jp).

Experimental setup for MEG experiment

The MEG experimental setting is shown in Supplementary Fig. 2A. Participants lay supine in a magnetically shielded room. We used a microcontroller system (Arduino Uno R3, SparkFun Electronics, USA) and optical fiber for precise timing control of the flash (see "Measurement of system delay" in Supplementary Methods). Button presses by the right middle, left index, and left middle fingers were recorded to the microcontroller board. Button presses by the right middle finger were also recorded to the MEG system through channels for external devices. A visual stimulus (flash) was produced by a light-emitting diode (LED) attached to the microcontroller, and it was shown to participants via an optic fiber extended to the center of the semi-transparent screen in front of the participant's face in the shielded room. The center of the screen was indicated by a virtual crossing point of three white lines (the "inverted T"; Supplementary Fig. 2B). The line below the crossing point was omitted to save space for showing task instructions (such as "press" and "judgment"). An auditory stimulus was sent to participants through an air tube. White noise was played via an air-tube headphone during the entire experiment to block the sound of button presses so that participants could not perceive the timing of the button presses by listening. Vertical and horizontal electro-oculogram (EOG) data were recorded to detect blinks and eye movements. Electromyogram (EMG) data were recorded from two surface electrodes on the flexor digitorum superficialis (FDS) to detect muscle activities of the right middle finger. In our preliminary experiment, we compared EMG patterns evoked by the index finger to those evoked by the middle finger. We found that onsets of EMG for the middle finger could be more reliably detected than for the index finger. Thus, we asked participants to use the middle finger in our voluntary button-press task (see below).

Tasks for participants in MEG experiment

Voluntary button-press task. Participants were asked to press a button with their right middle finger at their own pace and focus on the flash as the visual feedback of action outcome. The flash appeared as soon as the button was pressed (<0.4 ms, see "Measurement of system delay" in Supplementary Methods) in the no-delay condition (Fig. 1B) or 150 ms after the button press in the delay condition (Fig. 1A). The duration of flash was 50 ms. Participants were not informed about the lag of the flash during the experiment. Participants briefly practiced at pressing the button in random intervals between 5 and 10 s before the experiment.

Temporal order judgment task. For psychophysical measurement of the lag adaptation effect in individuals, voluntary button-press tasks (Fig. 1A and B) were followed by a temporal order judgment task (Fig. 1C). Participants responded to an auditory cue (frequency: 880 Hz, duration: 100 ms) as quickly as possible by pressing the same button with their right middle finger. Then participants reported whether the button press was earlier or later than the flash by pressing one of two buttons with their left index or middle finger. The software kept a running average of each participant's reaction time to the auditory cues given so far, making it possible to probabilistically place flashes just before or after the button press. The flash onsets were determined by a Gaussian distribution centered on 60 ms after the average response time with a standard deviation of 80 ms to maximize the number of trials at the steep part of the psychometric functions (e.g., Fig. 1D). This procedure followed a previous study on recalibration of motor-sensory asynchrony (Stetson et al., 2006).

Procedures of MEG experiment

Supplementary Fig. 3 shows the procedures of the MEG experiment. Before MEG measurement, there were sessions of response time measurement and training of temporal order judgment (Supplementary

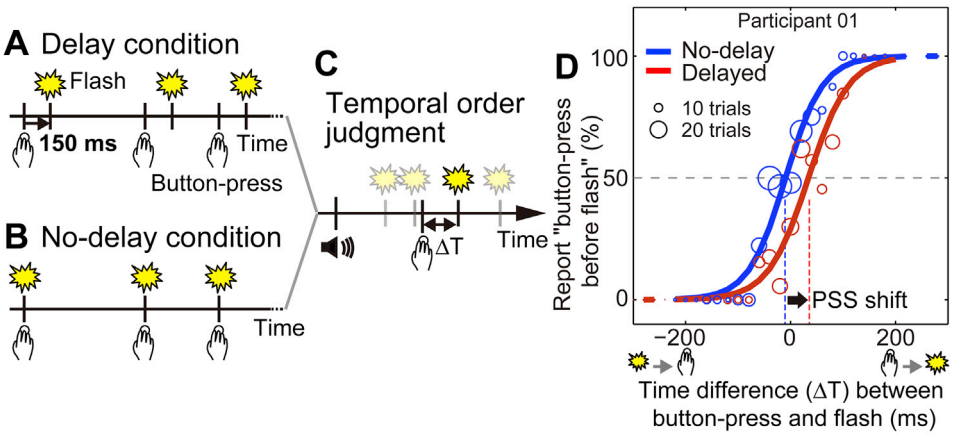

Fig. 1. Experimental procedure and psychophysical data.
(A, B, C) Temporal relationship between button press and flash in delay (A) and no-delay (B) conditions in voluntary button-press task as well as subsequent temporal order judgment task (C). See also Supplementary Fig. 3 for detailed experimental procedure.
(D) Behavioral results of temporal order judgment task for a representative participant after voluntary button-press task (blue for no-delay and red for delay conditions). See also Supplementary Fig. 5 for results of the other participants. Circle size represents the number of trials. PSS, point of subjective simultaneity.

Fig. 3A) to familiarize participants with the temporal order judgment task. In the response time measurement session, participants were asked to respond to the auditory cue as quickly as possible by pressing the button with their right middle finger.

Each participant completed 6–10 MEG sessions (Supplementary Fig. 3B), depending on the time available for the experiment (3 or 4.5 h) and the time the participant needed to rest between sessions. In each MEG session, there were two consecutive blocks with an inter-block interval of 2 s. Each block included a voluntary button-press task under the delay or no-delay condition (mean = 28.2 trials, SD = 2.9; one press, one trial) followed by a temporal order judgment task with two-thirds the number of trials (mean = 18.1 trials, SD = 1.6; one judgment, one trial) as the preceding voluntary button-press task according to a previous study (Stetson et al., 2006). Instructions of "press" and "judgment" were alternatively shown just below the center of the screen (Supplementary Fig. 2B) to inform participants of the current task (voluntary button-press task or temporal order judgment task, respectively). The no-delay and delay sessions were assigned to the first or second half of the MEG experiment to avoid frequent switching between adaptation and de-adaptation. The order of no-delay and delay sessions was counterbalanced across participants. See "MEG data acquisition" in Supplementary Methods for measurement details.

We told participants to avoid excessive eye movements as much as possible in the voluntary button-press task. During the entire experiment, participants were required to focus on the center of the screen, indicated by the virtual crossing point of the three white lines (Supplementary Fig. 2B).

Behavioral data analysis in temporal order judgment task in MEG experiment

Adaptation effects were measured behaviorally from the temporal order judgment task, which was commonly conducted in both the no-delay and delay sessions. To evaluate the lag adaptation effects in individuals, the degree to which the participants shifted their point of subjective simultaneity (PSS) was evaluated as in previous studies (Stetson et al., 2006; Tanaka et al., 2011). First, the timing between button press and flash in the temporal order judgment task was binned into 20-ms intervals between −300 and 300 ms. In each bin, we computed the probability that each participant judged the button press before visual flash feedback. Next, a sigmoid function, $F(x) = 1/(1 + exp(-(x-t0)/b))$, was fitted to the probability using a Matlab (MathWorks, Natick, MA, USA) *glmfit* function (Fig. 1D). Here, x is the time interval between button press and flash. The intercept $t0$ is taken as the PSS, and b represents the slope. As reported in the previous study (Stetson et al., 2006), adaptation to delayed flashes was expected to manifest itself as a shift of the PSS in the direction of the exposure lag. The PSS shift in the present study was incorporated in a correlation analysis with the shifts in readiness currents and visually evoked currents.

Cortical currents estimation by the hierarchical Bayesian method

We preprocessed MEG sensor signals ("Preprocessing of MEG data" in Supplementary Methods) measured during the voluntary button-press task and constructed an inverse filter that maps MEG sensor signals to cortical currents using a Variational Bayesian Multimodal EncephaloGraphy (VBMEG) method (Sato et al., 2004). As prior information for the Bayesian filter, we used fMRI data when participants pressed a button and observed a flash as a button-press consequence (see "fMRI experiment and data analysis" in Supplementary Methods). We followed the methods for cortical current estimation used in previous studies (Aihara et al., 2012; Morioka et al., 2014; Shibata et al., 2008; Toda et al., 2011; Yoshioka et al., 2008) (see "Cortical currents estimation" in Supplementary Methods). Specifically, cortical currents in the voluntary button-press task were estimated at about 20,000 vertices of a polygon model of the cortical surface for each participant in the delay and no-delay conditions (Supplementary Fig. 4). The estimated cortical currents remained at the same level of sampling frequency (100 Hz) and the same epochs (3 s before and 1 s after EMG onset, see "Preprocessing of MEG data" in Supplementary Methods) as the MEG resampled sensor data. The 3-s data before movement (EMG) onset were used for readiness current analysis; the data of 200 ms before and 600 ms after onset of the LED flash were used for visually evoked current analysis.

Search for vertices of readiness currents

To find vertices of readiness currents, we identified currents that exponentially increased in amplitude toward the movement onsets from among all vertices. First, we investigated the cortical current waveforms across trials as follows. We averaged the cortical currents (3 s, 300 time points) before movement (EMG) onset at each vertex across trials within each condition (no-delay or delay) separately for each participant and rectified them. Then we subtracted the mean current value in a period from 3 to 2.5 s before the EMG onset from the rectified currents. Finally, we temporally smoothed the resulting current with a low-pass filter with a cutoff frequency of 1 Hz.

As a second step, we used a dual-exponential function to fit the cortical current waveforms of the no-delay condition:

$$y_{no-delay}(t) = a \cdot \exp(b \cdot t) + c \cdot \exp(d \cdot t). \quad (1)$$

Here, t is the time from 3 s to 0 s before the movement onset, and a, b, c, and d are fitting parameters. The dual-exponential fitting followed the early and late components of readiness potentials (Shibasaki and Hallett, 2006). Cortical currents in the no-delay condition ($y_{no\text{-}delay}$) at each

vertex before movement onset were fitted with function (1) using the curve-fitting toolbox of Matlab with constraints of $b > 0$ and $d > 0$.

We also tried a Gaussian fitting, a one-term exponential fitting, and a linear-plus-exponential fitting. As a result, we found the dual-exponential fitting was superior to these fittings as evaluated by the determination coefficient (*adjusted* R^2, see "Calculation of determination coefficient" in Supplementary Methods) and Akaike's Information Criterion (see "Comparing dual-exponential fitting with other fitting methods" in Supplementary Methods).

Localizing readiness current distribution

Our group analysis of the readiness current distribution was carried out in three steps. First, we calculated the adjusted determination coefficients (*adjusted* R^2: see "Calculation of determination coefficient" in Supplementary Methods) of all vertices on the individual cortical surface by fitting a dual-exponential function (Eq. (1)) to currents in the no-delay condition. Second, the estimated R^2s were spatially morphed (normalized) onto the template cortical surface model "fsaverage" from FreeSurfer using the tool provided by VBMEG. The details of the normalization are described in the VBMEG manual (http://vbmeg.atr.jp/docs/manual/manual_e.html#toc32). Third, the normalized individual R^2s were spatially smoothed (Gaussian kernel size = 8 mm). If the normalized and smoothed individual R^2 exceeded 0.5 for more than 87.5% (14/16) of the total participants at a given vertex, this vertex was assumed to be involved in the readiness current area.

Because we mainly focus on the readiness currents in regions related to motor intention and preparation (Haggard, 2008; Lau et al., 2004; Shibasaki and Hallett, 2006; Wheaton et al., 2005; Wise et al., 1997), we restricted our region of interests (ROIs) within the common areas among BA 6, parietal cortex (superior and inferior parietal lobules), and the distribution of readiness current in the further analysis of shifts in readiness currents. We used WFU PickAtlas (http://fmri.wfubmc.edu/cms/software) for anatomical definitions of BA 6 and the parietal cortex.

Estimation of readiness current shifts

To get a temporal shift of the currents after lag adaptation at a readiness current vertex, we fitted the preprocessed currents of delay condition (y_{delay}) to a dual-exponential function with the same parameters a, b, c and d estimated from $y_{no\text{-}delay}$ fitting (Eq. (1)) by adding a time translation Δt to Eq. (1) as follows:

$$y_{delay}(t) = a \cdot \exp(b \cdot (t - \Delta t)) + c \cdot \exp(d \cdot (t - \Delta t)). \quad (2)$$

We estimated Δt in areas on the individual cortical surface corresponding to the readiness current area identified by the above group analysis. The estimated Δt values were normalized to the "fsaverage" template as done with the adjusted determination coefficient R^2 (Eq. (1) fitting) above. The normalized individual shifts were spatially smoothed (Gaussian kernel size = 8 mm) and converted to a surface image data format named GIFTI (http://www.nitrc.org/projects/gifti) for multi-participant analysis (see below).

Statistical analysis of readiness current shifts

For surface-based group analysis of readiness current shift (Δt), we used SPM12b (Wellcome Department of Cognitive Neurology, London, UK; http://www.fil.ion.ucl.ac.uk/spm/). Specifically, we assumed that Δt is determined by the summation of a constant component (α) and a variable component (β) correlated with the size of individual PSS shift. Then we conducted a linear regression analysis using the following equation for each vertex across participants:

$$\Delta t_i = \alpha + \beta \cdot \text{PSS shift}_i. \quad (3)$$

Here, Δt_i is the shift of a readiness current for the i-th participant, α is the intercept, and β is the slope of the regression analysis. If a region was identified as $\alpha > 0$, this meant that the readiness currents in this region were constantly delayed during lag adaptation; if a region was identified as $\beta > 0$, this meant that the shifts of readiness currents in the region during lag adaptation were positively correlated with the PSS shift (a psychophysical measure of the adaptation effect).

Our statistical threshold of planned contrasts was corrected for multiple comparisons based on Random Field Theory (Worsley et al., 1996) within the common areas among BA 6, the parietal cortex, and the distribution of readiness current (see above). We identified significant clusters at $P < 0.05$ FWE-corrected with a cluster-forming threshold of $P < 0.001$, uncorrected. We also checked regions showing trends of current shifts using a liberal threshold ($P < 0.05$ FWE-corrected at peak- or cluster-level with a cluster-forming threshold of $P < 0.01$, uncorrected).

Analysis of visually evoked currents

We analyzed the currents evoked by the action outcome (flash) within the occipital lobe (BA 17/18/19, defined by WFU PickAtlas), in which the cortical sources of visually evoked potentials have been localized (Celesia et al., 1982; Di Russo et al., 2002; Ikeda et al., 1998). The currents were aligned to the flash onset with a time window of 200 ms before and 600 ms after it. The sampling rate of evoked current was the same as readiness current (100 Hz). The evoked currents in each vertex were low-pass filtered at 30 Hz and averaged within delay and no-delay conditions. Then, the averaged cortical currents were baseline corrected by subtracting the mean of evoked current from 0 to 200 ms before the flash onset. These procedures followed previous studies on visually evoked potentials (Mayhew et al., 2012; Qian et al., 2012).

Evoked current waveforms are complex and difficult to model by a simple (e.g., exponential) function. Thus, we used a cross-correlation method (Matlab function, *xcorr*) to calculate the evoked current shifts between the no-delay and delay conditions at each vertex within BA 17/18/19. The *xcorr* function measures the correlation between one discrete-time sequence (current of no-delay condition in our case) and shifted (lagged) copies of another sequence (current of delay condition) as a function of the lag. The lag corresponding to the maximum correlation (i.e., the lag at which the waveforms between the two conditions were best aligned) was considered to be the shift Δt between the currents of no-delay and delay conditions. At each vertex, the averaged and baseline-corrected currents from 0 to 600 ms after the flash onset in the two conditions were used for the cross-correlation calculation. Cross-correlation is suitable for detecting the lag between two non-monotonic signals (such as visually evoked currents) with peaks or troughs, but is difficult for monotonic signals (such as readiness currents).

The statistical analysis of visually evoked current shifts was the same as that used for readiness current shifts. Evoked current shifts at individual vertices were normalized, smoothed and converted into GIFTI surface images. The regression analysis (Eq. (3)) was performed using SPM12b to identify regions where evoked current shift was constant (PSS-independent, $\alpha > 0$ or $\alpha < 0$) and regions where the shift was dependent on a PSS shift ($\beta > 0$ or $\beta < 0$) within BA 17/18/19. We identified significant clusters at $P < 0.05$ FWE-corrected with a cluster-forming threshold of $P < 0.001$, uncorrected.

Analysis of somatosensory evoked currents

Previous psychophysical studies (Di Luca et al., 2009; Keetels and Vroomen, 2008) suggest that shifts of timing in tactile and proprioceptive perception might contribute to motor-sensory calibration. We analyzed cortical current shifts from no-delay to delay condition within the contralateral somatosensory cortex (BA 1/2/3). Here, we followed the same data analysis procedures as done in visually evoked currents, except that we aligned the cortical currents to the timing when the button was pressed.

Results

Behavioral results of temporal order judgment task

A temporal order judgment task (Fig. 1C) following voluntary button-press tasks (Fig. 1A and B) was used for psychophysical measurement of the adaptation effect. We computed the probability that each participant judged the button press before the visual flash feedback after each condition and fitted a sigmoid function to this probability (see Fig. 1D for a representative participant and Supplementary Fig. 5 for the other participants). PSS shift from the no-delay to delay condition was significant across participants (mean ± SD: 18.63 ± 27.21 ms, $P = 0.02$, $t(15) = 2.74$, a one-sample t-test, two-tailed), but the magnitude of the shift was variable depending on participants as shown in Supplementary Fig. 5. We did not find a significant difference in slope of the sigmoid function at 50% probability between the conditions ($P = 0.75$, $t(30) = -0.32$, a paired t-test, two-tailed).

Readiness current analysis results

We identified readiness current vertices in which the currents exponentially increased in amplitude toward the movement onsets in the no-delay condition (Eq. (1)). The fitted data and actual data in the no-delay condition are shown in Supplementary Fig. 6. The values for the fitted parameters for all participants are shown in Supplementary Table 1. As readiness current areas, we determined vertices at which the waveform was well fitted by the exponential function ($R^2 \geq 0.5$) for more than 14 of the total 16 participants (>87.5%, Fig. 2A). The readiness current areas included left motor, premotor cortex, and parietal cortex, but not the supplementary motor areas (SMA, including pre-SMA).

The distribution of the temporal shift of readiness currents (Δt) from the no-delay to the delay condition within the readiness current area across participants is shown in Fig. 2B. The median and average of Δt was 3.6 ms and 61.0 ms (SD = 287.6 ms), respectively. The distribution, with a heavy tail in the positive value, was not a normal distribution (Kolmogorov-Smirnov test, $P < 1.0 \times 10^{-10}$). The median of Δt was significantly larger than 0 (Wilcoxon signed-rank test, $P < 1.0 \times 10^{-10}$). These data show a trend to a later shift of readiness currents from the no-delay to the delay condition.

We tested the statistical significance of the constant effect on Δt at each readiness current vertex across participants (α in Eq. (3)). Fig. 3A shows areas where the readiness current constantly shifted later in the delay than in the no-delay condition ($\alpha > 0$) within the common areas among BA 6, the parietal cortex (enclosed by dotted gray lines), and the readiness current area (Fig. 2A). We corrected the P-value for multiple comparisons within the common area and found a significant shift in BA 40 (yellow; $P < 0.05$, family-wise error (FWE)-corrected with a cluster-forming threshold of $P < 0.001$, uncorrected; Table 1). We also found a trend to a later shift in the dorsal premotor (PMd in BA 6) and other parietal regions (dark red; $P < 0.05$, FWE-corrected with a cluster-forming threshold of $P < 0.01$, uncorrected). The average shift was 219.9 ± 290.4 ms (mean ± SD) within the significant shift area in BA 40 (yellow area in Fig. 3A). Fig. 3B shows the waveforms between the conditions averaged across participants at vertices within BA 40.

We also tested the statistical significance of the variable effect (β in Eq. (3)) on Δt, which means the correlation between the cortical current shift at each readiness current vertex and the shift of PSS across participants. Fig. 3C shows an area where the readiness current shift was significantly and positively correlated with the PSS shift on an individual basis ($\beta > 0$; $P < 0.05$ FWE-corrected with a cluster-forming threshold of $P < 0.001$, uncorrected). We simultaneously estimated coefficients for the constant shift (α) and the shift correlated with the PSS shift (β) using one linear regression model (Eq. (3)). Fig. 3D shows a scatter plot of the averaged readiness current shifts (yellow region in Fig. 3C) and PSS shifts across participants. Since the readiness current shifts occurred prior to sensory feedback, these results cannot be explained by retrospective sensory recalibration but instead support the hypothesis of prospective processing in motor-related circuits.

We found no vertex of a significant advance ($\alpha < 0$) or a negative correlation with the PSS shift ($\beta < 0$) ($P < 0.05$ FWE-corrected with a cluster-forming threshold of $P < 0.01$, uncorrected). There was no significant difference in the current-peak maximum (searched from 3 s before to 1 s after movement onset) averaged within the areas of Fig. 3A between the conditions (paired Wilcoxon signed-rank test, $P = 0.92$). We recorded EMG from muscles related to the right middle finger (see Materials and methods) and found no significant difference in the EMG-peak maximum between the conditions (paired Wilcoxon signed-rank test, $P = 0.21$).

Visually evoked current analysis results

We analyzed the temporal shifts in the currents evoked by a flash (evoked currents) in the occipital visual cortex (BA 17/18/19). The evoked current shift was -20.4 ± 99.7 ms (mean ± SD) averaged across the visual cortex and participants (Fig. 4). The distribution, with a heavy tail in the negative value, was not a normal distribution (Kolmogorov-Smirnov test, $P < 1.0 \times 10^{-10}$). The median shift was −9.4 ms, which was significantly smaller than 0 (Wilcoxon signed-rank test, $P < 1.0 \times 10^{-10}$). The negative value means that the evoked current shifted earlier in the delay than in the no-delay condition. We applied the same regression analysis as Eq. (3) to the individual evoked current shifts at each vertex across participants. Fig. 5A shows areas where the early shift of evoked currents was significant ($\alpha < 0$; $P < 0.05$ FWE-

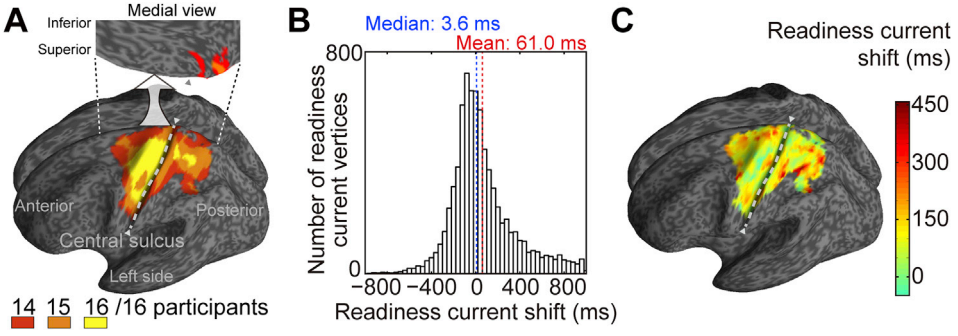

Fig. 2. Readiness current areas and shifts.
(A) Colored regions indicate where the readiness currents were identified in more than 87.5% (14/16) of the participants. Medial view of readiness currents areas in the left hemisphere is shown in the upper callout illustration. The dotted gray line indicates the central sulcus on the left hemisphere.
(B) Histogram of readiness current shifts (Δt) within the area shown in (A) for all participants. These Δt values were pooled across participants. Each bin represents 40 ms. The median, mean and standard deviation of Δt is 3.6 ms (dotted blue line), 61.0 ms (dotted red line), and 287.6 ms, respectively. See also Supplementary Fig. 7 for illustration of readiness current shifts.
(C) Spatial distribution of averaged readiness current shifts (Δt) across all participants. The areas in red show where the readiness currents in delay condition increase later than currents in no-delay condition; the areas in green show where the readiness currents in delay condition increase earlier than currents in no-delay condition. Note that Δt values were pooled in (B) but averaged in (C) across participants for each readiness current vertex.

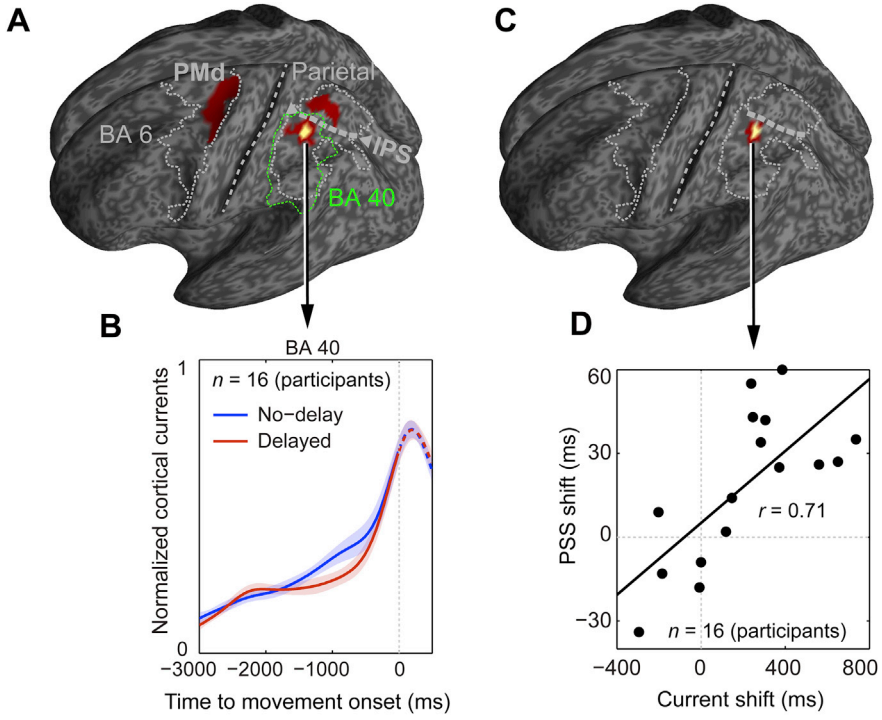

Fig. 3. Statistical results of readiness current shifts.
(A) Yellow region indicates where a constant delay in the readiness current due to lag adaptation was significant across the participants ($P < 0.05$ FWE-corrected at peak- and cluster-level with a cluster-forming threshold of $P < 0.001$, uncorrected) within the fronto-parietal network (BA 6 and parietal cortex, outlined by thin dotted gray lines). Dark-red regions in PMd and parietal cortex indicate a tendency of the current delay ($P < 0.05$ FWE-corrected at peak- or cluster-level with a cluster-forming threshold of $P < 0.01$, uncorrected). BA 40 is outlined by a thin dotted green line. BA, Brodmann area; IPS, intraparietal sulcus; PMd, dorsal premotor region.
(B) Average of normalized readiness currents within BA 40 (yellow) clusters in (A). Shaded bands indicate the ranges of the standard error of the mean (SEM) across all participants. Note that the readiness current waveforms were aligned to the movement onset (0 ms, an electromyogram onset, see "Preprocessing MEG data" in Supplementary Methods) and that the current shift was calculated from −3000 to 0 ms (solid curves).
(C) In this parietal region of BA 40, there is a significant correlation between the shifts of the readiness current and the point of subjective simultaneity (PSS) (yellow, $P < 0.05$ FWE-corrected at peak- and cluster-level with a cluster-forming threshold of $P < 0.001$, uncorrected). Dark-red regions indicate a tendency of correlation ($P < 0.05$ FWE-corrected at cluster-level with a cluster-forming threshold of $P < 0.01$, uncorrected).
(D) Scatter plot showing correspondence between the averaged shifts of the readiness current within the yellow region in (C) and the PSS shifts across participants. Each circle corresponds to each participant.

Table 1
Clusters showing significant shifts in readiness and evoked currents due to lag adaptation.[a]

	BA	Peak coordinates[b]			Cluster Size[c]	*T*-value at peak[d]	*P*-value FWE-corrected[e]	
		x	*y*	*z*			at cluster level	at peak level
Readiness current with constant delay (Fig. 3A, yellow)								
L parietal region	40	−34	−46	46	5	4.55	**0.034**	**0.020**
Readiness current delay correlated with PSS shift (Fig. 3C, yellow)								
L parietal region	40	−34	−46	46	4	4.45	**0.039**	**0.024**
Visually evoked current with constant advance (Fig. 5A)								
(1) R occipital lobe	17/18/19	28	−68	28	75	9.73	**<0.001**	**<0.001**
(2) R occipital lobe	17/18/19	20	−74	32	24	5.02	**0.010**	0.090
(3) L occipital lobe	17/18	−8	−92	−10	15	4.92	**0.047**	0.103
(4) R occipital lobe	17/18	8	−66	2	16	4.53	**0.040**	0.179

BA, Brodmann area; PMd, dorsal premotor; L, left; R, right; Bold *P*-values, $P < 0.05$ FWE-corrected.
[a] Cluster-forming threshold set at $P < 0.001$, uncorrected.
[b] Montreal Neurological Institute coordinates.
[c] Number of vertices in each cluster.
[d] We also conducted a nonparametric analysis (Winkler et al., 2014) and confirmed that the significant current-shift peaks survived correction with the FWE rate ($P < 0.05$).
[e] Readiness current results were corrected for multiple comparisons within the common areas between readiness current areas (Fig. 2A) and left fronto-parietal network (BA 6 and parietal cortex, enclosed by thin dotted gray lines in Fig. 3A); visually evoked current results were corrected within visual cortex (BA 17/18/19).

corrected within the visual cortex, Table 1). Such areas were mainly found in BA 19 and partly in BA 17/18. Fig. 5B shows the averaged evoked current shifts within the above areas for all participants (-49.7 ± 25.0 ms, mean ± SD). Fig. 5C shows evoked current waveforms for representative participants averaged within a 10-mm-radius sphere around the highest peak (1) in Fig. 5A. The advanced evoked current shifts in the visual cortex show that retrospective sensory processing also contributes to the motor-sensory asynchrony recalibration. We found no vertex at which evoked currents were significantly delayed ($\alpha > 0$) or their shifts were correlated with an individual PSS shift ($\beta > 0$ or $\beta < 0$) within the visual cortex ($P < 0.05$ FWE-corrected with a cluster-forming threshold of $P < 0.01$, uncorrected).

Somatosensory evoked current analysis results

We analyzed cortical current shifts from no-delay to delay condition within the contralateral somatosensory cortex (BA 1/2/3) following the data analysis procedures as done for visually evoked currents. We found no vertex or cluster showing a trend of significant advance ($\alpha < 0$) or delay ($\alpha > 0$) shifts ($P < 0.05$ FWE-corrected at cluster-forming threshold $P < 0.01$, uncorrected).

Discussion

Our results indicate that readiness currents shift later while visually

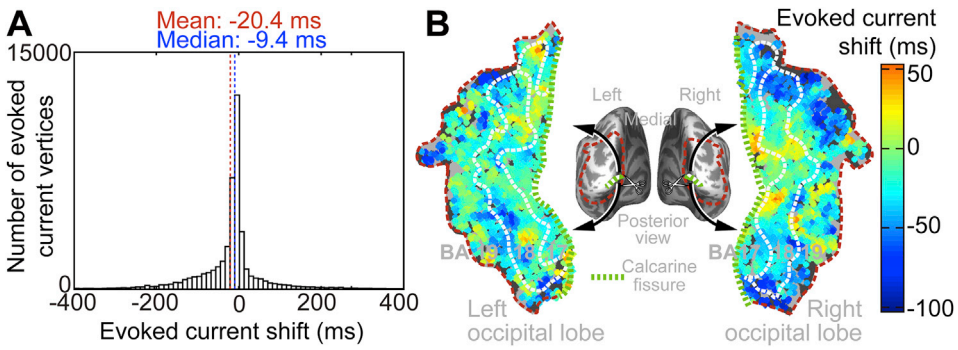

Fig. 4. Shifts of visually evoked current in the occipital lobe.
(A) Histogram of visually evoked current shifts (Δt) within BA 17/18/19 for all participants. The shifts (Δt) were pooled across participants. Each bin represents 10 ms. The median, mean and standard deviation of Δt is −9.4 ms (dotted blue line), −20.4 ms (dotted red line), and 99.7 ms, respectively. Positive shifts mean evoked currents shifted later in delay condition than in no-delay condition, and negative shifts mean evoked currents shifted earlier in delay condition.
(B) Spatial distribution of averaged evoked current shifts (Δt) across all participants on flat maps of the left and right occipital lobes. Each colored dot represents one vertex. The areas in blue show where the evoked currents in delay condition shift earlier than in no-delay condition. Note that Δt-values were pooled in (A) but averaged in (B) across participants for each evoked current vertex. BA 17, 18, and 19 are separated by white dotted lines.

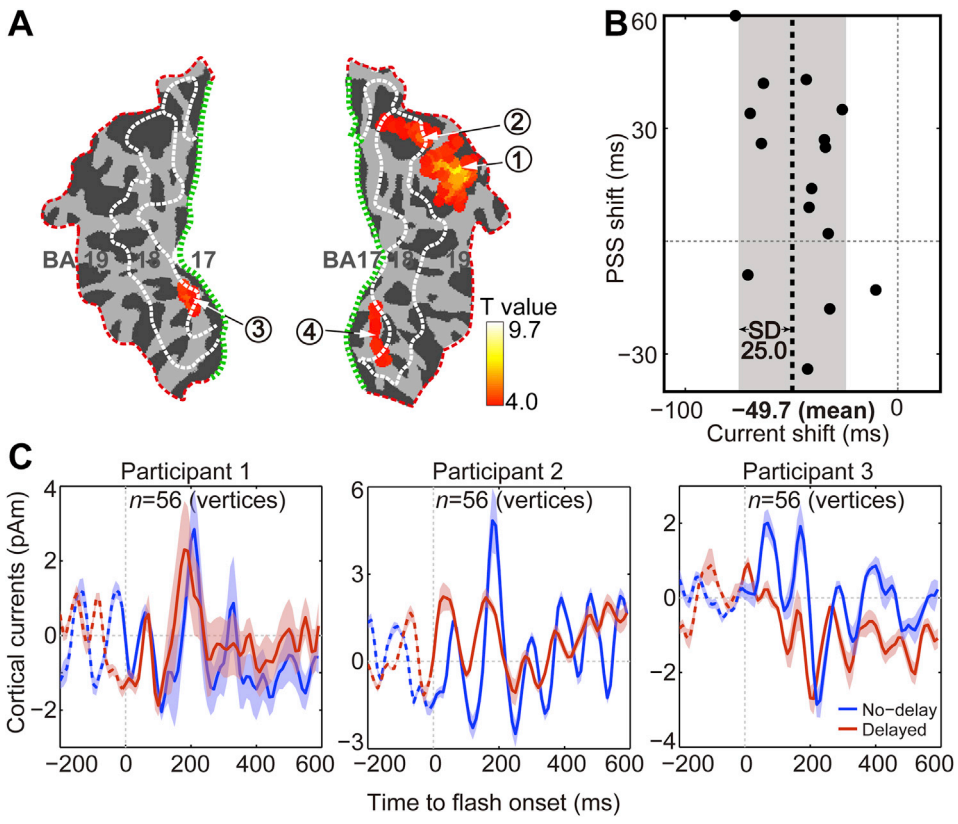

Fig. 5. Statistical results of visually evoked current shifts.
(A) Red/orange/yellow regions indicate clusters where an earlier evoked current shift was significant across the participants ($P < 0.05$ FWE-corrected, see Table 1 for details). The circled numbers identify the clusters and the white arrows show the locations of peak shifts on flat maps of the left and right occipital lobes (conventions follow Fig. 4B).
(B) Scatter plot of averaged evoked current shifts (−49.7 ± 25.0 ms, mean ± SD) within the red/orange/yellow regions shown in (A) and the point of subjective simultaneity (PSS) shifts across participants.
(C) Temporal plots of the mean evoked currents from the vertices centered at the peak in cluster (1) in (A) within the 10-mm-radius sphere for three participants. The shaded bands indicate the ranges of the SEM of the evoked currents across vertices. Note that the evoked current waveforms were aligned to the flash onset (0 ms) and the evoked current shift was calculated from 0 to 600 ms (solid curves).

evoked currents shift earlier due to lag adaptation in voluntary movements. These shifts are congruent with shifts in the perceived timing of an action and its outcome in the intentional binding effect (Haggard et al., 2002). It is known that our awareness of movement is derived from signals that precede the movements rather than sensory feedback from the moving limb (Blakemore and Frith, 2003; Libet et al., 1983). Such signals have been localized in parietal regions: An electrical stimulation in the parietal region including BA 40 evokes intention or awareness of movements even without actual movement (Desmurget et al., 2009). Later shifts of readiness currents in this region reflect delayed awareness (perceived timing) of action. A correlation between shifts in PSS and readiness currents in BA 40 (Fig. 3C and D) confirms the relevance of this region to motor awareness before movements. A larger shift in readiness current than in PSS (see axis ratio in Fig. 3D) is consistent with previous findings that a large change at the neural level is necessary to induce a change at the conscious level, e.g., a minimum duration of 500 ms is required for an electric stimulation in the somatosensory cortex to elicit a conscious sensation (Libet et al., 1964).

In the present study, no consistent readiness current distribution was identified within SMA, including the pre-SMA regions (Fig. 3A), which have been related to the source of readiness potentials (Haggard, 2008; Shibasaki and Hallett, 2006). Although some studies reported current dipoles correlated with readiness potentials in SMA, it has been suggested that MEG has difficulty in detecting the radially orientated dipoles in SMA due to cancelation of bilateral dipoles (Shibasaki and Hallett, 2006). It is known that SMA is bilaterally activated even by ipsilateral hand movement (Nguyen et al., 2014). This may be a reason why we were unable to identify readiness current in SMA.

Regarding the earlier shift in visually evoked currents (Figs. 4 and 5) in lag adaptation, convergent findings suggest that neurons in the early

visual cortex receive inputs from other cortical areas, such as the parietal regions, and that their activity is modulated by the states of these other regions (Muckli and Petro, 2013). Recent studies found that motor-related signals modulate visual response in the mouse visual cortex, suggesting predictive coding of visual information depending on the behavioral state (Keller et al., 2012; Niell and Stryker, 2010). As for human studies, it is known that the peak of visual potentials in the primary visual cortex shifts earlier when attention is paid to visual stimuli compared to when no attention is paid to them (Vibell et al., 2007). Thus, a shift of cortical currents is not implausible, even in the primary visual cortex, due to the lag adaptation. Since the higher visual cortex likely has more connections with other regions than does the primary cortex, it is reasonable that the shift of evoked currents is more prominent in BA 19 than in BA 17/18.

Although our data cannot conclusively identify the precise neural mechanism of temporal recalibration, we would go so far as to conjecture that the observed shifts in readiness current and visually evoked current reflect temporal learning in an internal predictive model. Our data suggest that both shifts are based on prediction of the delay imposed between the action and its consequence for the following reasons. First, the shift of readiness current occurs in the prospective process before the movement initiation (Fig. 3B). Second, the shift of the visually evoked currents in the delayed condition was found immediately after the flash onset (Fig. 5C). This suggests predictive modulation of the currents before the sensory event rather than reflective modulation after recognition of the delay. Studies on human motor control have suggested that the central nervous system acquires internal models of control objects and environments for predictive control of movements (Flanagan and Wing, 1997; Kawato, 1999; Wolpert et al., 1995). Although many studies have intensively investigated internal models of kinematic and dynamic properties of objects and environments (e.g., Imamizu et al., 2000; Shadmehr and Holcomb, 1997), an important factor in predictive motor control is the ability to learn the temporal difference between the timing of a control signal and that of the corresponding feedback. A theoretical study (Miall et al., 1993) has proposed the hypothesis that the cerebellum acquires an internal model of the feedback delay (but also see Miall and Jackson, 2006). Unfortunately, our study did not investigate currents in the cerebellum due to the technical difficulties in estimating current within that region. Further studies are needed on the neural mechanisms used by an internal model of feedback delay that might have induced the later shift of readiness current and the earlier shift of visually evoked current.

In the present study, we investigated the neural signatures for motor-sensory synchrony within voluntary movements, which is a critical issue for the sense of agency and conscious awareness of action (Blakemore and Frith, 2003; Haggard, 2005). There is an inevitable delay of feedback in man-machine interfaces such as a car-driving system and remote control of robot hands. Our methods can objectively evaluate the degree to which users adapt to the feedback delay of an interface by investigating shifts of the readiness and sensory-evoked potentials. Since electroencephalography (EEG) can also measure both potentials, our methods can be used in natural and realistic environments using EEG rather than MEG. As an example of clinical application, we note that schizophrenia has a subset of symptoms, including delusions of control, delusions of thought-insertion, and third-person auditory hallucinations. All of these symptoms have been conceptualized as reflecting the difficulty in distinguishing between internally and externally generated events (Frith, 1992). One study investigated EEG signals of schizophrenia patients when they pressed a button to elicit an auditory stimulus (Whitford et al., 2011). The patients exhibited weak suppression of the evoked potential to self-generated auditory stimuli, but a significant suppression was observed when imposing a 50-ms delay between the button press and the stimulus. This suggests that prediction of action consequence is temporally delayed in the patients, which leads to the difficulty in distinguishing between internally and externally generated events. Our methods can be applied to investigate whether the prospective process (i.e., the readiness potential) in schizophrenia is altered from that in healthy controls. If so, it would be worthwhile to examine whether neurofeedback training could induce a temporal shift of the readiness potential and ameliorate the above symptoms in schizophrenia.

Conclusions

Although further studies are needed to elucidate how the earlier shift in visually evoked currents was induced (i.e., mechanisms for the temporal binding between motor- and sensory-related processes), we approach the prospective/retrospective controversy by providing the first neural evidence, to our knowledge, that both the prospective motor system and the retrospective visual system recalibrate asynchronous action and vision in voluntary movements. When considering the larger shifts in the motor system, and the significant positive correlation between shifts in the parietal cortex and the psychophysical measure of lag adaptation, the prospective motor processing seems to play the major role in motor-sensory asynchrony recalibration.

Conflicts of interest

The authors declare that there is no conflict of interest.

Acknowledgements

This work was partially supported by JSPS KAKENHI 26120002 (H.I.), 25430007 (H.T.) and 26120005 (H.T), “Development of BMI Technologies for Clinical Application” of SRPBS-MEXT (H.I.), and ImPACT Cabinet Office of Japan (H.I.). We thank Shin'ya Nishida, Masaaki Sato, Okito Yamashita, Taku Yoshioka, Satoshi Tada, Yuka Furukawa, Kaori Nakamura, Nobuo Hiroe, Eiichi Naito, and Gowrishankar Ganesh for technical advice and support. We also thank Shigeru Kitazawa and Nobuhiro Hagura for comments on an early draft of this manuscript.

Appendix A. Supplementary data

Supplementary data related to this article can be found at https://doi.org/10.1016/j.neuroimage.2018.02.015.

References

Aihara, T., Takeda, Y., Takeda, K., Yasuda, W., Sato, T., Otaka, Y., Hanakawa, T., Honda, M., Liu, M., Kawato, M., Sato, M.A., Osu, R., 2012. Cortical current source estimation from electroencephalography in combination with near-infrared spectroscopy as a hierarchical prior. Neuroimage 59, 4006–4021.

Blakemore, S.J., Frith, C., 2003. Self-awareness and action. Curr. Opin. Neurobiol. 13, 219–224.

Cai, M., Stetson, C., Eagleman, D.M., 2012. A neural model for temporal order judgments and their active recalibration: a common mechanism for space and time? Front. Psychol. 3, 470.

Celesia, G.G., Polcyn, R.D., Holden, J.E., Nickles, R.J., Gatley, J.S., Koeppe, R.A., 1982. Visual evoked potentials and positron emission tomographic mapping of regional cerebral blood flow and cerebral metabolism: can the neuronal potential generators be visualized? Electroencephalogr. Clin. Neurophysiol. 54, 243–256.

Desmurget, M., Reilly, K.T., Richard, N., Szathmari, A., Mottolese, C., Sirigu, A., 2009. Movement intention after parietal cortex stimulation in humans. Science 324, 811–813.

Di Luca, M., Machulla, T.K., Ernst, M.O., 2009. Recalibration of multisensory simultaneity: cross-modal transfer coincides with a change in perceptual latency. J. Vis. 9 (7), 1–16.

Di Russo, F., Martinez, A., Sereno, M.I., Pitzalis, S., Hillyard, S.A., 2002. Cortical sources of the early components of the visual evoked potential. Hum. Brain Mapp. 15, 95–111.

Flanagan, J.R., Wing, A.M., 1997. The role of internal models in motion planning and control: evidence from grip force adjustments during movements of hand-held loads. J. Neurosci. 17, 1519–1528.

Frith, C.D., 1992. The Cognitive Neuropsychology of Schizophrenia. Lawrence Erlbaum Associates, Hove, UK.

Haggard, P., 2005. Conscious intention and motor cognition. Trends Cognit. Sci. 9, 290–295.

Haggard, P., 2008. Human volition: towards a neuroscience of will. Nat. Rev. Neurosci. 9, 934–946.

Haggard, P., 2014. Intention and agency. In: Gazzaniga, M.S., Mangun, G.R. (Eds.), The Cognitive Neurosciences. MIT Press, Cambridge MA, pp. 875–885.
Haggard, P., Clark, S., Kalogeras, J., 2002. Voluntary action and conscious awareness. Nat. Neurosci. 5, 382–385.
Ikeda, H., Nishijo, H., Miyamoto, K., Tamura, R., Endo, S., Ono, T., 1998. Generators of visual evoked potentials investigated by dipole tracing in the human occipital cortex. Neuroscience 84, 723–739.
Imamizu, H., Miyauchi, S., Tamada, T., Sasaki, Y., Takino, R., Putz, B., Yoshioka, T., Kawato, M., 2000. Human cerebellar activity reflecting an acquired internal model of a new tool. Nature 403, 192–195.
Kawato, M., 1999. Internal models for motor control and trajectory planning. Curr. Opin. Neurobiol. 9, 718–727.
Keetels, M., Vroomen, J., 2008. Temporal recalibration to tactile-visual asynchronous stimuli. Neurosci. Lett. 430, 130–134.
Keller, G.B., Bonhoeffer, T., Hubener, M., 2012. Sensorimotor mismatch signals in primary visual cortex of the behaving mouse. Neuron 74, 809–815.
Kornhuber, H.H., Deecke, L., 1965. Changes in the brain potential in voluntary movements and passive movements in man: readiness potential and reafferent potentials. Pflugers Arch. Gesamte Physiol. Menschen Tiere 284, 1–17.
Lau, H.C., Rogers, R.D., Haggard, P., Passingham, R.E., 2004. Attention to intention. Science 303, 1208–1210.
Libet, B., Alberts, W.W., Wright Jr., E.W., Delattre, L.D., Levin, G., Feinstein, B., 1964. Production of threshold levels of conscious sensation by electrical stimulation of human somatosensory cortex. J. Neurophysiol. 27, 546–578.
Libet, B., Gleason, C.A., Wright, E.W., Pearl, D.K., 1983. Time of conscious intention to act in relation to onset of cerebral activity (readiness-potential). The unconscious initiation of a freely voluntary act. Brain 106 (Pt 3), 623–642.
Mayhew, S.D., Li, S., Kourtzi, Z., 2012. Learning acts on distinct processes for visual form perception in the human brain. J. Neurosci. 32, 775–786.
Miall, R.C., Jackson, J.K., 2006. Adaptation to visual feedback delays in manual tracking: evidence against the Smith Predictor model of human visually guided action. Exp. Brain Res. 172, 77–84.
Miall, R.C., Weir, D.J., Wolpert, D.M., Stein, J.F., 1993. Is the cerebellum a smith predictor? J. Mot. Behav. 25, 203–216.
Moore, J., Haggard, P., 2008. Awareness of action: inference and prediction. Cons. Cogn. 17, 136–144.
Morioka, H., Kanemura, A., Morimoto, S., Yoshioka, T., Oba, S., Kawanabe, M., Ishii, S., 2014. Decoding spatial attention by using cortical currents estimated from electroencephalography with near-infrared spectroscopy prior information. Neuroimage 90, 128–139.
Muckli, L., Petro, L.S., 2013. Network interactions: non-geniculate input to V1. Curr. Opin. Neurobiol. 23, 195–201.
Nguyen, V.T., Breakspear, M., Cunnington, R., 2014. Reciprocal interactions of the SMA and cingulate cortex sustain premovement activity for voluntary actions. J. Neurosci. 34, 16397–16407.
Niell, C.M., Stryker, M.P., 2010. Modulation of visual responses by behavioral state in mouse visual cortex. Neuron 65, 472–479.
Qian, C., Al-Aidroos, N., West, G., Abrams, R.A., Pratt, J., 2012. The visual P2 is attenuated for attended objects near the hands. Cognit. Neurosci. 3, 98–104.
Sato, M.A., Yoshioka, T., Kajihara, S., Toyama, K., Goda, N., Doya, K., Kawato, M., 2004. Hierarchical Bayesian estimation for MEG inverse problem. Neuroimage 23, 806–826.
Shadmehr, R., Holcomb, H.H., 1997. Neural correlates of motor memory consolidation. Science 277, 821–825.
Shibasaki, H., Hallett, M., 2006. What is the Bereitschaftspotential? Clin. Neurophysiol. 117, 2341–2356.
Shibata, K., Yamagishi, N., Goda, N., Yoshioka, T., Yamashita, O., Sato, M.A., Kawato, M., 2008. The effects of feature attention on prestimulus cortical activity in the human visual system. Cerebr. Cortex 18, 1664–1675.
Stetson, C., Cui, X., Montague, P.R., Eagleman, D.M., 2006. Motor-sensory recalibration leads to an illusory reversal of action and sensation. Neuron 51, 651–659.
Sugano, Y., Keetels, M., Vroomen, J., 2010. Adaptation to motor-visual and motor-auditory temporal lags transfer across modalities. Exp. Brain Res. 201, 393–399.
Tanaka, H., Homma, K., Imamizu, H., 2011. Physical delay but not subjective delay determines learning rate in prism adaptation. Exp. Brain Res. 208, 257–268.
Toda, A., Imamizu, H., Kawato, M., Sato, M.A., 2011. Reconstruction of two-dimensional movement trajectories from selected magnetoencephalography cortical currents by combined sparse Bayesian methods. Neuroimage 54, 892–905.
Vibell, J., Klinge, C., Zampini, M., Spence, C., Nobre, A.C., 2007. Temporal order is coded temporally in the brain: early event-related potential latency shifts underlying prior entry in a cross-modal temporal order judgment task. J. Cognit. Neurosci. 19, 109–120.
Wheaton, L.A., Nolte, G., Bohlhalter, S., Fridman, E., Hallett, M., 2005. Synchronization of parietal and premotor areas during preparation and execution of praxis hand movements. Clin. Neurophysiol. 116, 1382–1390.
Whitford, T.J., Mathalon, D.H., Shenton, M.E., Roach, B.J., Bammer, R., Adcock, R.A., Bouix, S., Kubicki, M., De Siebenthal, J., Rausch, A.C., Schneiderman, J.S., Ford, J.M., 2011. Electrophysiological and diffusion tensor imaging evidence of delayed corollary discharges in patients with schizophrenia. Psychol. Med. 41, 959–969.
Winkler, A.M., Ridgway, G.R., Webster, M.A., Smith, S.M., Nichols, T.E., 2014. Permutation inference for the general linear model. Neuroimage 92, 381–397.
Wise, S.P., Boussaoud, D., Johnson, P.B., Caminiti, R., 1997. Premotor and parietal cortex: corticocortical connectivity and combinatorial computations. Annu. Rev. Neurosci. 20, 25–42.
Wolpert, D.M., Ghahramani, Z., Jordan, M.I., 1995. An internal model for sensorimotor integration. Science 269, 1880–1882.
Worsley, K.J., Marrett, S., Neelin, P., Vandal, A.C., Friston, K.J., Evans, A.C., 1996. A unified statistical approach for determining significant signals in images of cerebral activation. Hum. Brain Mapp. 4, 58–73.
Yoshioka, T., Toyama, K., Kawato, M., Yamashita, O., Nishina, S., Yamagishi, N., Sato, M.A., 2008. Evaluation of hierarchical Bayesian method through retinotopic brain activities reconstruction from fMRI and MEG signals. Neuroimage 42, 1397–1413.